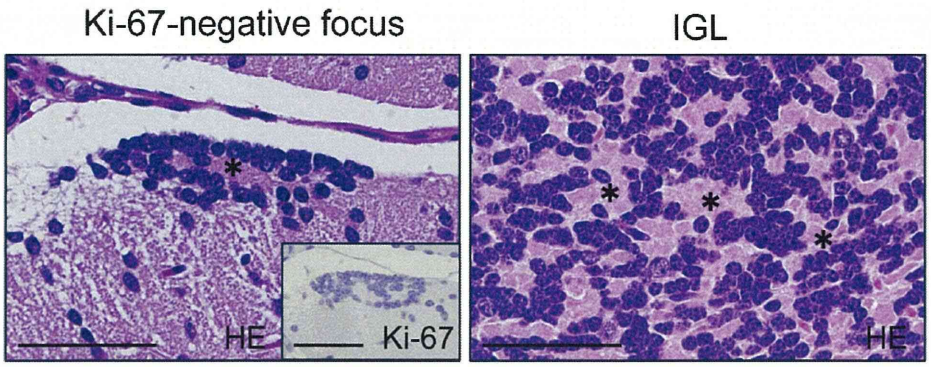

Fig. 8. Ki-67-negative foci showing differentiation into the IGL. HE staining of Ki-67-negative focus (left) and the IGL (right) of Ptch1 mice at PND21. An eosinophilic mossy fiber-like substance (asterisk) was surrounded by nuclei of Ki-67-negative focus. Mossy fibers (asterisk) were observed among the nuclei of granular cells of the IGL. Scale bar: 50 μm.

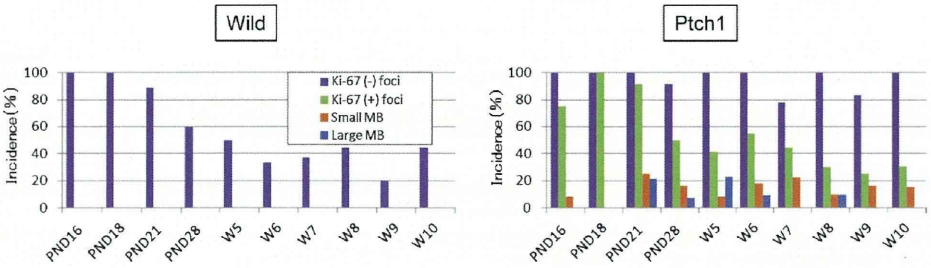

Fig. 9. Incidences of Ki-67-negative (−) and positive (+) foci and MBs in wild-type and Ptch1 mice. Incidences (%) were calculated as follows: number of animals which have specific lesion (e.g. Ki-67-negative foci) in the cerebellum relative to the total number of animals examined. Ki-67-negative foci were observed in both genotypes, but in higher incidence in Ptch1 mice throughout the examination period. The incidence of Ki-67-positive foci had a tendency to decrease with aging. Incidences of small MB and large MB had no tendency to increase with aging.

4. Discussion

The present study was performed to clarify derived cell and early changes of MBs in Ptch1 mice using immunohistochemistry. We also compared cerebellar developmental processes in Ptch1 mice to wild-type mice. Currently, human MBs are classified as four distinct subtypes by molecular studies (Ellison et al., 2011; Northcott et al., 2011; Jones et al., 2012; Kool et al., 2012). Tumors of Ptch1 mice are thought to be equivalent for those of the Shh subgroup in human (Lau et al., 2012). Therefore, MBs in Ptch1 mice will be good tool for testing new drugs targeting the Shh pathway. Additionally, detailed investigation of the cerebellar development and early changes of MB in Ptch1 mice will be beneficial to understanding pathogenesis of human MBs.

During the experimental period, Ptch1 mice showed no clinical signs except development of hydrocephalus and rhabdomyosarcomas in some cases, an outcome that has been previously described (Corcoran and Scott, 2001; Wetmore et al., 2000; Svärd et al., 2009). Although the pathogenesis of hydrocephalus in Ptch1 mice has not been fully understood, impaired cilia function of the ependymal cells might be related (Gavino and Richard, 2011).

The present study demonstrated that a single injection of BrdU was useful in pursuing the sequential migrating process of GCPs from the EGL to the IGL. Similar to results of another study (Thomas et al., 2009), we observed that the migration process in Ptch1 mice was the same as that in wild-type mice and that the proliferation of GCPs increased in Ptch1 mice resulting in a slightly wider EGL layer. No clear evidence was obtained, but the increased proliferation in the EGL in Ptch1 mice might be related to the high potential for MB described below. Shh signaling regulates the expansion of the pool of GCPs (Roussel and Hatten, 2011; Wang et al., 2012). Reduced levels of Ptch1 expression in the cerebellum of Ptch1 mice might be caused by loss of one allele resulting in increased proliferation of GCPs (Corcoran and Scott, 2001; Goodrich et al., 1997; Gupta et al., 2010; Toftgard, 2000; Yang et al., 2008). In addition, an extended duration of GCP localization in the EGL might increase opportunities for additional mutations which may lead to tumorigenesis (Corcoran and Scott, 2001; Wetmore et al., 2000).

Proliferative lesions such as preneoplastic lesions of MBs during 3 weeks after birth in Ptch1 mice were described as rare occurrences in previous reports (Kim et al., 2003); however, our detailed and sequential examination revealed that proliferative lesions and MBs had already been detected in Ptch1 mice within 3 weeks after birth. The morphology and immunohistochemistry of MBs at PND12 indicated that MBs arose from GCPs of the outer layer of the EGL during cerebellar development. The cells of the earliest proliferative lesion, focal thickened area of the EGL, showed the same immunohistochemical profiles as GCPs of the outer layer of the EGL.

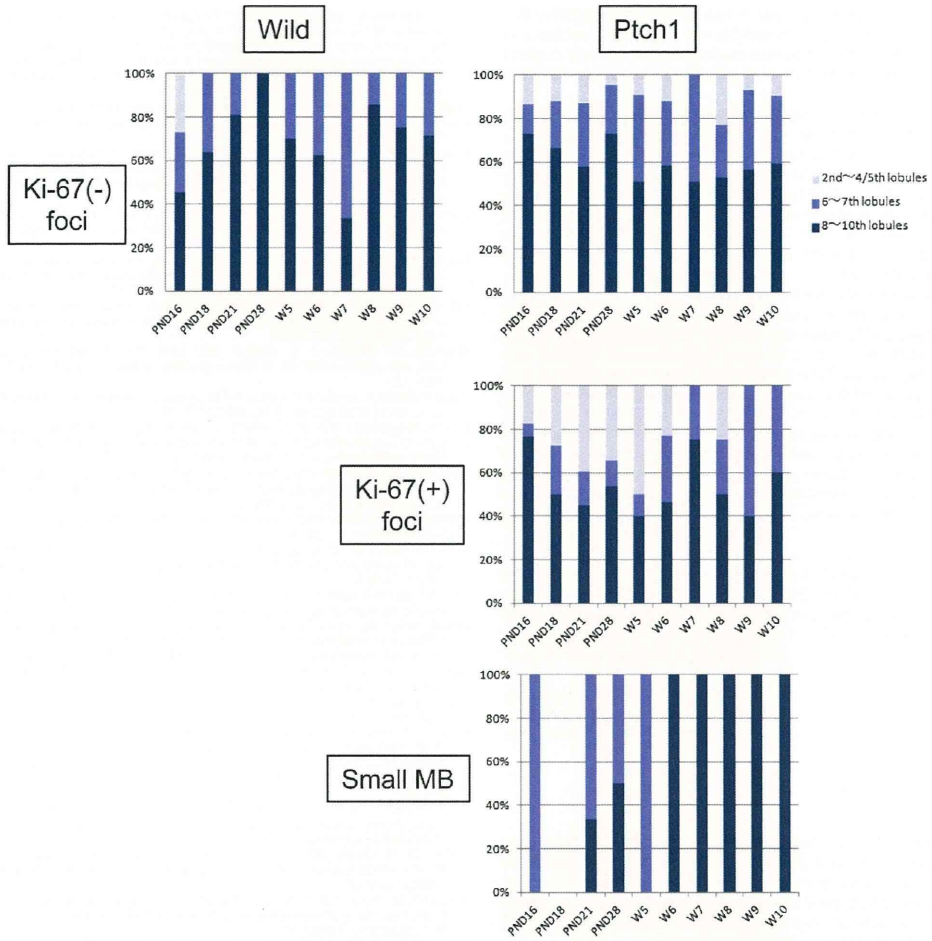

Fig. 10. Location of Ki-67-negative (−) and positive (+) foci and small MBs in the cerebellum of wild-type and Ptch1 mice. Incidences (%) were calculated as follows: total number of specific lesion per cerebellar lobule of all animal examined relative to total number of the lesion in the whole cerebellum of all animals examined.

As the thickened area had cellular atypia and disarrangement compared to normal GCPs, it was considered to be preneoplastic of MB. The appearance of focal thickened proliferative lesions was limited during PND10 to PND14 when the EGL was detectable in this study. It may be that those lesions were recognized as Ki-67-positive foci or small MBs after PND16 because normal GCPs neighboring the lesions disappeared due to migration into the IGL after PND16.

We also found another preneoplastic lesion of MB derived from residual GCPs as Ki-67-positive focus only in Ptch1 mice. In previous reports, MBs were thought to arise from residual GCPs located at the surface of the cerebellum (Corcoran and Scott, 2001; Goodrich et al., 1997). In our study, the foci of GCP-like cells were found on the surface of the cerebellar cortex and only detectable on and after PND16. They were clearly divided into two types by the morphological and immunohistochemical profiles and genotypes. Observation of the EGL in BrdU-treated animal revealed that both types of the foci with BrdU-positive cells were composed of residual GCPs. The cells of Ki-67 positive foci had the same profiles as granular cells of the outer layer of the EGL, indicating that they were undifferentiated and had high proliferating potential. The other focus, Ki-67-negative type, was composed of cells showing neuronal differentiation with a lack of proliferating activity. They resembled granular cells of the IGL or the inner layer of the EGL indicating that the cells were already differentiated into mature granular cells. The Ki-67-negative foci were detected in both genotypes. In addition, more than half of the Ki-67-positive foci were located in the 6–10th lobules of the cerebellum as well as in small MBs in Ptch1 mice. Although MBs are thought to be derived from residual GCPs located in the EGL of the cerebellum (Behesti and Marino, 2009; Roussel and Hatten, 2011), these results strongly suggest that residual GCPs in the Ki-67-positive

foci were preneoplastic lesions. A high yield of Ki-67-positive foci may be useful as an easily detectable and confidential indicator of MB. These preneoplastic lesions might be useful as early markers to detect modulation effects of chemicals to shorten experimental periods.

The observation of a higher incidence of Ki-67-negative foci in Ptch1 mice as compared to wild-type mice and a reduced incidence of Ki-67-negative foci with increased age in wild-type mice was unexpected. These findings may be attributable to smaller Ki-67-negative foci in wild-type mice and a much lower number per animal as compared to Ptch1 mice, although their incidences were 100%. Chances to find the foci in a cross section of the cerebellum may have been reduced with increased age in wild-type mice due to cerebellar growth.

Purkinje cells secrete the mitogen Shh for GCP proliferation in the EGL during early phases of cerebellar development (Roussel and Hatten, 2011). After the GCPs lost cell proliferating activity, they migrate along radial fibers of Bergmann glia (Roussel and Hatten, 2011). It has been reported that abnormal development of Purkinje cells and Bergmann glia can disrupt proliferation, migration, and differentiation of GCPs (Adams et al., 2002; D'Arca et al., 2010; Rakic and Sidman, 1973; Schwartz et al., 1997). Our immunohistochemical results demonstrate no abnormal morphology in Bergmann glia or Purkinje cells, indicating that the MB formation process during cerebellar development might be intrinsic to the GCPs rather than abnormalities in Bergmann glia and Purkinje cells.

In conclusion, a thickened area of the EGL and Ki-67-positive foci were considered to be the early preneoplastic lesions of MBs derived from GCPs in the EGL in Ptch1 mice. These were distinguishable by immunohistochemistry with proliferation and neuronal differentiation markers. Preneoplastic lesions of MBs may serve as useful indicators and as substitutions for advanced MBs in the evaluation of drug efficacy and modulating effects of additional gene mutations, chemicals, and irradiation. Importantly, the Ki-67-positive focus is an easily detectable and confidential indicator due to higher occurrences in the third week after birth.

Acknowledgements

We thank Tomomi Morikawa for technical assistance in conducting the study and genotyping, and Miss Ayako Kaneko for technical assistance in histopathological preparation. This study was partly supported by Health and Labor Sciences Research Grants, Research on Risk of Chemical Substances, Ministry of Health, Labor and Welfare (H22-Toxicol-003).

References

Adams NC, Tomoda T, Cooper M, Dietz G, Hatten ME. Mice that lack astrotactin have slowed neuronal migration. Development 2002;129:965–72.
Aref D, Moffatt CJ, Agnihotri S, Ramaswamy V, Dubuc AM, Northcott PA, et al. Canonical TGF-beta pathway activity is a predictor of SHH-driven medulloblastoma survival and delineates putative precursors in cerebellar development. Brain Pathology 2012.
Ayrault O, Zindy F, Rehg J, Sherr CJ, Roussel MF. Two tumor suppressors, p27Kip1 and patched-1, collaborate to prevent medulloblastoma. Molecular Cancer Research 2009;7:33–40.
Behesti H, Marino S. Cerebellar granule cells: insights into proliferation, differentiation, and role in medulloblastoma pathogenesis. The International Journal of Biochemistry and Cell Biology 2009;41:435–45.
Bhatia B, Potts CR, Guldal C, Choi S, Korshunov A, Pfister S, et al. Hedgehog-mediated regulation of PPARγ controls metabolic patterns in neural precursors and shh-driven medulloblastoma. Acta Neuropathologica 2012;123:587–600.
Briggs KJ, Corcoran-Schwartz IM, Zhang W, Harcke T, Devereux WL, Baylin SB, et al. Cooperation between the Hic1 and Ptch1 tumor suppressors in medulloblastoma. Genes and Development 2008;22:770–85.
Corcoran RB, Scott MP. A mouse model for medulloblastoma and basal cell nevus syndrome. Journal of Neuro-Oncology 2001;53:307–18.
Crawford JR, MacDonald TJ, Packer RJ. Medulloblastoma in childhood: new biological advances. The Lancet Neurology 2007;6:1073–85.
D'Arca D, Zhao X, Xu W, Ramirez-Martinez NC, Iavarone A, Lasorella A. Huwe1 ubiquitin ligase is essential to synchronize neuronal and glial differentiation in the developing cerebellum. Proceedings of the National Academy of Sciences of the United States of America 2010;107:5875–80.
Dhall G. Medulloblastoma. Journal of child neurology 2009;24:1418–30.
Dyer MA. Mouse models of childhood cancer of the nervous system. Journal of clinical pathology 2004;57:561–76.
Ecke I, Rosenberger A, Obenauer S, Dullin C, Aberger F, Kimmina S, et al. Cyclopamine treatment of full-blown Hh/Ptch-associated RMS partially inhibits Hh/Ptch signaling, but not tumor growth. Molecular carcinogenesis 2008;47:361–72.
Ellison DW, Dalton J, Kocak M, Nicholson SL, Fraga C, Neale G, et al. Medulloblastoma: clinicopathological correlates of SHH WNT, and non-SHH/WNT molecular subgroups. Acta Neuropathologica 2011;121:381–96.
Farioli-Vecchioli S, Tanori M, Micheli L, Mancuso M, Leonardi L, Saran A, et al. Inhibition of medulloblastoma tumorigenesis by the antiproliferative and pro-differentiative gene PC3. FASEB Journal 2007;21:2215–25.
Gavino C, Richard S. Patched1 haploinsufficiency impairs ependymal cilia function of the quaking viable mice, leading to fatal hydrocephalus. Molecular and Cellular Neurosciences 2011;47:100–7.
Goodrich LV, Milenkovic L, Higgins KM, Scott MP. Altered neural cell fates and medulloblastoma in mouse patched mutants. Science 1997;277:1109–13.
Gupta S, Takebe N, Lorusso P. Targeting the Hedgehog pathway in cancer. Therapeutic Advances in Medical Oncology 2010;2:237–50.
Hahn H, Wojnowski L, Miller G, Zimmer A. The patched signaling pathway in tumorigenesis and development: lessons from animal models. Journal of Molecular Medicine (Berlin, Germany) 1999;77:459–68.
Haldipur P, Bharti U, Govindan S, Sarkar C, Iyengar S, Gressens P, et al. Expression of Sonic hedgehog during cell proliferation in the human cerebellum. Stem Cells and Development 2012;21:1059–68.
Hatten ME, Roussel MF. Development and cancer of the cerebellum. Trends in Neurosciences 2011;34:134–42.
Huse JT, Holland EC. Targeting brain cancer: advances in the molecular pathology of malignant glioma and medulloblastoma. Nature Reviews Cancer 2010;10:319–31.
Jones DT, Jager N, Kool M, Zichner T, Hutter B, Sultan M, et al. Dissecting the genomic complexity underlying medulloblastoma. Nature 2012;488:100–5.
Kim JY, Nelson AL, Algon SA, Graves O, Sturla LM, Goumnerova LC, et al. Medulloblastoma tumorigenesis diverges from cerebellar granule cell differentiation in patched heterozygous mice. Developmental Biology 2003;263:50–66.
Kimura H, Stephen D, Joyner A, Curran T. Gli1 is important for medulloblastoma formation in $Ptc1^{+/-}$ mice. Oncogene 2005;24:4026–36.
Klesse LJ, Bowers DC. Childhood medulloblastoma: current status of biology and treatment. CNS Drugs 2010;24:285–301.
Kool M, Korshunov A, Remke M, Jones DT, Schlanstein M, Northcott PA, et al. Molecular subgroups of medulloblastoma: an international meta-analysis of transcriptome, genetic aberrations, and clinical data of WNT, SHH, Group 3, and Group 4 medulloblastomas. Acta Neuropathologica 2012;123:473–84.
Lau J, Schmidt C, Markant SL, Taylor MD, Wechsler-Reya RJ, Weiss WA. Matching mice to malignancy: molecular subgroups and models of medulloblastoma. Child's Nervous System 2012;28:521–32.
Mohan AL, Friedman MD, Ormond DR, Tobias M, Murali R, Jhanwar-Uniyal M. PI3K/mTOR signaling pathways in medulloblastoma. Anticancer Research 2012;32:3141–6.
Northcott PA, Korshunov A, Witt H, Hielscher T, Eberhart CG, Mack S, et al. Medulloblastoma comprises four distinct molecular variants. Journal of Clinical Oncology 2011;29:1408–14.
Oliver TG, Read TA, Kessler JD, Mehmeti A, Wells JF, Huynh TT, et al. Loss of patched and disruption of granule cell development in a pre-neoplastic stage of medulloblastoma. Development 2005;132:2425–39.
Pazzaglia S. Ptc1 heterozygous knockout mice as a model of multi-organ tumorigenesis. Cancer Letters 2006;234:124–34.
Pazzaglia S, Pasquali E, Tanori M, Mancuso M, Leonardi S, di Majo V, et al. Physical, heritable and age-related factors as modifiers of radiation cancer risk in patched heterozygous mice. International Journal of Radiation Oncology, Biology, Physics 2009;73:1203–10.
Pazzaglia S, Tanori M, Mancuso M, Gessi M, Pasquali E, Leonardi S, et al. Two-hit model for progression of medulloblastoma preneoplasia in Patched heterozygous mice. Oncogene 2006;25:5575–80.
Pogoriler J, Millen K, Utset M, Du W. Loss of cyclin D1 impairs cerebellar development and suppresses medulloblastoma formation. Development 2006;133:3929–37.
Raffel C. Medulloblastoma: molecular genetics and animal models. Neoplasia 2004;6:310–22.
Rakic P, Sidman RL. Weaver mutant mouse cerebellum: defective neuronal migration secondary to abnormality of Bergmann glia. Proceedings of the National Academy of Sciences of the United States of America 1973;70:240–4.
Roussel MF, Hatten ME. Cerebellum development and medulloblastoma. Current Topics in Developmental Biology 2011;94:235–82.
Schwartz PM, Borghesani PR, Levy RL, Pomeroy SL, Segal RA. Abnormal cerebellar development and foliation in $BDNF^{-/-}$ mice reveals a role for neurotrophins in CNS patterning. Neuron 1997;19:269–81.

Svärd J, Rozell B, Toftgard R, Teglund S. Tumor suppressor gene co-operativity in compound Patched1 and suppressor of fused heterozygous mutant mice. Molecular Carcinogenesis 2009;48:408–19.
Takahashi M, Matsuo S, Inoue K, Tamura K, Irie K, Kodama Y, et al. Development of an early induction model of medulloblastoma in Ptch1 heterozygous mice initiated with N-ethyl-N-nitrosourea. Cancer Science 2012;103:2051–5.
Thomas WD, Chen J, Gao YR, Cheung B, Koach J, Sekyere E, et al. Patched1 deletion increases N-Myc protein stability as a mechanism of medulloblastoma initiation and progression. Oncogene 2009;28:1605–15.
Toftgard R. Hedgehog signalling in cancer. Cellular and Molecular Life Sciences 2000;57:1720–31.
Uziel T, Zindy F, Xie S, Lee Y, Forget A, Magdaleno S, et al. The tumor suppressors Ink4c and p53 collaborate independently with Patched to suppress medulloblastoma formation. Genes and Development 2005;19:2656–67.
Wang X, Venugopal C, Manoranjan B, McFarlane N, O'Farrell E, Nolte S, et al. Sonic hedgehog regulates Bmi1 in human medulloblastoma brain tumor-initiating cells. Oncogene 2012;31:187–99.
Wetmore C, Eberhart DE, Curran T. The normal patched allele is expressed in medulloblastomas from mice with heterozygous germ-line mutation of patched. Cancer Research 2000;60:2239–46.
Wetmore C, Eberhart DE, Curran T. Loss of p53 but not ARF accelerates medulloblastoma in mice heterozygous for patched. Cancer Research 2001;61:513–6.
Wu X, Northcott PA, Croul S, Taylor MD. Mouse models of medulloblastoma. Chinese Journal of Cancer 2011;30:442–9.
Yang ZJ, Ellis T, Markant SL, Read TA, Kessler JD, Bourboulas M, et al. Medulloblastoma can be initiated by deletion of Patched in lineage-restricted progenitors or stem cells. Cancer Cell 2008;14:135–45.

The Journal of Toxicological Sciences (J. Toxicol. Sci.)
Vol.38, No.6, 891-902, 2013

Original Article

Effects of pyperonyl butoxide on the female reproductive tract in rats

Seigo Hayashi[1], Yoshikazu Taketa[1], Kaoru Inoue[1], Miwa Takahashi[1], Saori Matsuo[1], Kaoru Irie[1], Gen Watanabe[2] and Midori Yoshida[1]

[1]Division of Pathology, National Institute of Health Sciences, 1-18-1 Kamiyoga, Setagaya-ku Tokyo 158-8501, Japan
[2]Laboratory of Veterinary Physiology, Tokyo University of Agriculture and Technology, 3-5-8 Saiwai-cho, Fuchu-shi, Tokyo 183-8509, Japan

(Received July 30, 2013; Accepted September 11, 2013)

ABSTRACT — This study was investigated the effects of piperonyl butoxide (PBO) on the female reproductive tract. Female Crj:Donryu rats were fed a basal diet containing 5,000, 10,000 or 20,000 ppm PBO for 28 days, and compared with food-restricted rats of comparable body weights to those in the PBO 10,000 or 20,000 ppm groups. Although treatment with 20,000 ppm PBO for 28 days depressed body weight gain, the abnormal estrous cyclicity, mainly prolonged diestrus, was also induced by the PBO treatment which was not correlated with body weight change. 20,000 ppm PBO treatment markedly decreased uterine weights and slightly decreased ovarian weights. 10,000 and 20,000 ppm PBO treatment increased liver weights. These cycle and organ weight changes were linked to atrophic uterus and increased atretic follicles in the ovary. In hormone assays, PBO at both doses reduced serum E2 levels, but did not affect corticosterone levels. An anti-uterotrophic assay showed a slight but significant decrease in absolute uterine weight and a reduction of endometrial epithelium height in the 20,000 ppm group. PBO was positive in an ER α antagonist reporter gene assay, although the activity was much weaker than that of 4-hydroxytamoxifen. These results indicate that high-dose PBO treatment directly induces atrophic changes in the female reproductive tract in rats, and these effects are likely the result of a hypoestrogenic state and the anti-estrogenic activity of PBO.

Key words: Piperonyl butoxide, Female reproductive tract, Anti-uterotrophic assay, Reporter gene assay

INTRODUCTION

Piperonyl butoxide (PBO), α-[2-(2-butoxyethoxy) ethoxy]-4,5-methylenedioxy-2-propyltoluene, is a pesticide synergist that is widely used in combination with pyrethrins and synthetic pyrethroids. PBO acts as a synergist through acute inhibition of cytochrome P450, thereby reducing pesticide metabolism in the insect (Franklin, 1972). Sub-acute or chronic exposure to PBO in rodents, however, induces liver hypertrophy and increases cytochrome P450 activity (Butler *et al.*, 1998; Philips *et al.*, 1997). Furthermore, previous studies have shown that dietary exposure to 2.4% PBO also affects the female reproductive tract of F344 rats, resulting in decreased ovarian weight (Takahashi *et al.*, 1994) and uterine atrophy (Fujitani *et al.*, 1992). However, the mechanism by which these effects are induced by PBO remains unclear.

High-dose exposure to PBO is also reported to cause suppression of body weight gain in rats (Philips *et al.*, 1997; Fujitani *et al.*, 1992), which may potentially confound studies assessing its effects on reproduction. Feeding restriction with resultant body weight reduction affects reproductive function and reduces fertility in rats (Chapin *et al.*, 1993; Terry *et al.*, 2005). Therefore it is unclear whether the reproductive effects of PBO treatment are primary or secondary. In general, atrophy of the female reproductive tract induced by a chemical compound is caused by disruption of the hypothalamus-pituitary axis, ovarian dysfunction, and/or anti-estrogenic effects of the compound.

In the present study, we clarified the effects of PBO on the female reproductive tract in rats. We first focused on the question of whether the effects of PBO on the female

Correspondence: Midori Yoshida (E-mail: midoriy@nihs.go.jp)

reproductive tract are secondary to body weight change. We compared the effects of PBO on estrous cyclicity, reproductive organ weight, and serum hormone levels in PBO-treated rats and those with similar body weights induced by food restriction. To evaluate other possible causes of the effects of PBO on the female reproductive tract, we assessed the anti-estrogenic potential of PBO using both an anti-uterotrophic assay and an estrogen reporter gene assay.

MATERIALS AND METHODS

Chemicals

Piperonyl butoxide (PBO, CAS No. 51-03-6) and dimethyl sulfoxide (DMSO) were purchased from Wako Pure Chemical Industries (Osaka, Japan). 17β-estradiol (E2, CAS No. 50-28-2) was purchased from Sigma Aldrich (St. Louis, MO, USA). PBO was mixed with the powdered basal diet, CRF-1 (Oriental Yeast Co., Tokyo, Japan). Test diets were prepared every 2 weeks, and stored at 4°C before use.

Animals and housing conditions

Female Crj:Donryu rats bred in our laboratory were used in the present study. This rat strain has a regular four-day estrous cycle. They received the basal diet (CRF-1, Oriental Yeast) and tap water *ad libitum*, and were housed 2-3 per plastic cage with sterilized softwood chips as bedding in a barrier-maintained animal room, conditioned at 24 ± 1°C and 55 ± 5% humidity with a 12-hr light/dark cycle. All experimental protocols and animal use were reviewed and approved by the Animal Care and Utilization Committee of the National Institute of Health Science.

Experiment 1 (28-day feeding study of PBO)

6-week-old female rats were fed diets containing either 0, 5,000, 10,000 and 20,000 ppm of PBO for 28 days (10 animals/group). The PBO doses were determined based on previous reports that uterine atrophy was induced by 2.4% PBO treatment (Fujitani *et al.*, 1992), and effects on body weight gain were observed with 2% PBO treatment (Muguruma *et al.*, 2007). The rats were observed daily for clinical signs and mortality, and body weight was recorded twice a week. The amounts of supplied and residual diet were weighed twice a week in order to calculate the average daily consumption of PBO. To investigate the effect on weight gain, we included two food-restricted (FR) groups with weight changes comparable to those observed in the PBO 10,000 and 20,000 ppm groups (FR-1 and FR-2 respectively, each with eight animals). The animals were weighed daily and fed a weight-based basal diet in the mornings (FR-1: 13.3 g/day average, FR-2: 9.3 g/day average). Estrous cyclicity was checked by vaginal cytology in all animals in the morning (9:00-10:00) throughout the treatment period. To compare the effect on serum hormone levels and the morphological findings of the female reproductive tract between the control and other groups, the animals were euthanized by decapitation at proestrus (high E2 level) and diestrus. If the rats were acyclic or predominantly diestrus, these animals were sacrificed at these stages. Table 1 shows the number of animals at each of estrous stages at autopsy. After the treatment period, all rats were euthanized by decapitation, and trunk blood was collected. Serum samples were stored at -80°C until the hormonal assay. Serum concentrations of estradiol-17β (E2) and progesterone (P4) were determined by double-antibody radioimmunoassay (RIA) systems using ^{125}I-labeled radioligands, as described previously (Taya *et al.*, 1985). Serum concentrations of follicle stimulated hormone (FSH), luteinizing hormone (LH) and prolactin (PRL) were measured using National Institute of Diabetes and Digestive and Kidney Disease (NIDDK) radioimmunoassay kits for rat FSH, LH and PRL (NIAMDD, NIH, Bethesda, MD, USA) (Taya *et al.*, 1983). The serum concentration of immunoreactive inhibin-α was analyzed using a rabbit anti-serum against bovine inhibin (TNDH-1) and ^{125}I-labelled 32-kDa bovine inhibin, as described previously (Hamada *et al.*, 1989). After the macroscopic examination, the ova-

Table 1. Number of animals at each of estrous stages at autopsy (experiment 1)

	Pyperonyl butoxide in the diet (ppm)				FR-1	FR-2
	0	5,000	10,000	20,000		
No. of examined animals	10	10	10	10	8	8
Estrous stages						
Proestrus	5	5	6	0	3	4
Diestrus	5	5	4	10	5	4

ries, uterus, vagina, adrenals, pituitary, thymus and liver were removed and the weight of each was recorded. Immediately after weighing, the organs were fixed in 10% neutral buffered formalin, and routinely processed for paraffin embedding, sectioned and stained with hematoxylin and eosin (HE). For analysis of ovarian histopathology, ovaries were transversally halved at dissection at the point with the greatest cross-sectional area, and both sections were examined. For uterine histopathology, both the uterine horns and uterine cervix were examined in one section each. Morphological classification of the female reproductive tract at each estrous stage was in accordance with previous reports (Westwood, 2008; Yuan and Foley, 2002; Yoshida *et al.*, 2009).

Experiment 2 (Anti-uterotrophic assay)

Female rats were ovariectomized at 15 weeks of age, and randomly allocated to five treatment groups (5 animals/group). PBO treatment began 2 weeks postoperatively at the following doses: 0 (negative control; NC), 5,000, 10,000 and 20,000 ppm PBO in the diet and daily subcutaneous injection of E2 in DMSO at a dose of 1 μg/kg concurrently for 2 weeks. E2 was dissolved in DMSO to allow for dosing at 1 ml/kg body weight. The rats in the vehicle control (VC) group were fed the basal diet and were injected with DMSO in the same manner as the treated groups. Animals were weighed daily and food consumption was measured twice a week. After the treatment period, all animals were euthanized, and the wet and blotted uterine weights recorded. The uteri were fixed in 10% neutral buffered formalin, routinely processed for paraffin embedding, sectioned and stained with HE for histopathologic examination. The luminal epithelial cell height in the uterine horn was measured at 5 different locations per animal using an image analyzer, Image J (National Institutes of Health, Bethesda, Maryland, USA).

Experiment 3 (Reporter gene assay)

To assess for anti-estrogenic activity *in vitro*, a reporter gene assay employing human estrogen receptor (ERα) was performed by Chemicals Evaluation and Research Institute (Tokyo, Japan), as previously reported (Takesyoshi *et al.*, 2002a, 2002b).

Statistical analysis

Differences in final body weight, absolute and relative organ weights, serum hormone level and uterine epithelial cell height were examined. These data were analyzed using Bartlett's test or the F test. When variances were homogeneous, Dunnett's multiple comparison test or Student's t test was performed. Steel's multiple comparison test or Aspin-Welch t test was employed, when variances were not homogenous. The levels of significance were set at $P < 0.05$ and 0.01.

RESULTS

Experiment 1 (28-day feeding study of PBO)

Body weight

Fig.1 shows the body weight curves for the female rats treated with PBO. Weight loss occurred within the first seven days in the 20,000 ppm group, and within the first three days in the 10,000 ppm group. Both groups gradually gained weight thereafter. Body weight reduction in the FR-2 group was noted several days later than that in the 20,000 ppm group, and the reduction continued until day 17. Overall, the sequential changes in body weight in the FR-1 and FR-2 groups were similar to those in the matched PBO-treated groups. In the 5,000 ppm group, weight gain was slightly reduced during the study period. Final body weights of the 5,000, 10,000 and 20,000 ppm, FR-1, and FR-2 groups were 91, 87, 67, 87 and 68% of those in the control group, respectively.

Food consumption and chemical intake

The food consumption in each of the PBO treated groups was lower than that in the control group in the first 3 days; however, the difference was no longer evident from days 7-28 days (Fig. 2). The actual PBO intake of the 5,000, 10,000 and 20,000 ppm groups was 468.8, 1104.0 and 2394.8 mg/kg per day, respectively (Table 2).

Estrous cyclicity

All rats in the control group showed a regular 4-day estrous cycle throughout the treatment period (Fig. 3A). Five rats in the 20,000 ppm group showed prolonged die-

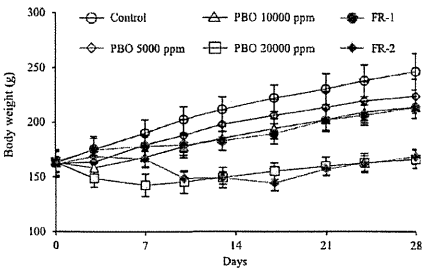

Fig. 1. Body weight curves in experiment 1 (mean ± S.D.).

Table 2. Achieves dose of PBO (experiment 1).

	Pyperonyl butoxide in diet (ppm)		
	5,000	10,000	20,000
No. of animals	10	10	10
Intake of PBO (mg/kg bw/day)	468.76 ± 83.01[a)]	1103.97 ± 205.94	2394.80 ± 446.01

[a)]Mean ± S.D.

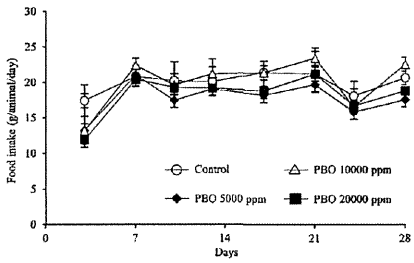

Fig. 2. Daily food intake in experiment 1 (mean ± S.D.).

strus, and the remaining rats in the same group cycled irregularly within 5 to 7 days of treatment initiation. The rats' estrous cyclicity remained abnormal for the duration of the experiment (Fig. 3B). In the FR-2 group, prolonged diestrus or cycle irregularity appeared on day 14, coincidental with the reduction in body weight. Estrous cyclicity normalized once body weight gain recovered to increase (Fig. 3C). The 5,000 and 10,000 ppm and FR-1 groups exhibited no estrous cycle disruption over the entire study period (data not shown).

Organ weights

Table 3 shows the organ weights of the PBO and FR groups. The most marked change in organ weight was the decrease in uterine weight at diestrus with 20,000 ppm PBO treatment. This group had uterine weights that were one-third the weights in the control group. In the FR-2 group, absolute uterine weights were slightly decreased, but relative uterine weights were slightly increased at both proestrus and diestrus. Absolute and relative weights of the ovaries and pituitary were slightly decreased in the 20,000 ppm group, but not in the FR2 group. Liver weights were significantly increased in the 10,000 and 20,000 ppm groups, but decreased in the FR2 group. Absolute but not relative weights of the adrenals and thymus were decreased in the PBO and FR groups.

Pathology findings

Macroscopically, marked uterine atrophy was noted in the 20,000 ppm group. Hepatic enlargement was observed in the 10,000 and 20,000 ppm groups. These changes correlated with the changes in the organ weights and his-

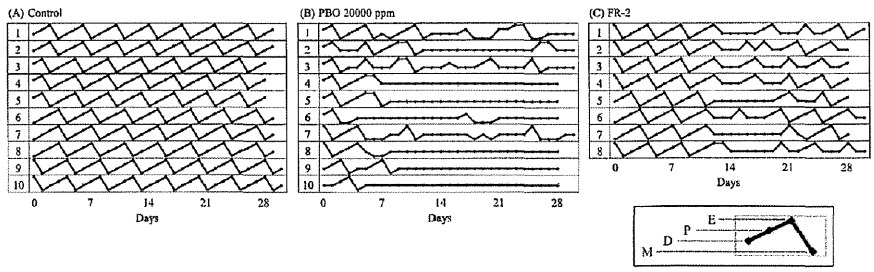

Fig. 3. Estrous cyclicity in experiment 1. (A) control group, (B) 20,000 ppm group, (C) FR-2 group. The plot for each animal is a four-level depiction of the estrus cycle: data points indicate each estrus stage illustrated in the right column (M: metestrus, D: diestrus, P: proestrus, E: estrus).

Table 3. Final body weight and organ weights (experiment 1).

	Pyperonyl butoxide in the diet (ppm)				FR-1	FR-2
	0	5,000	10,000	20,000		
No. of examined animals	10	10	10	10	8	8
Final B.W.(g)	246.6 ± 16.6[a)]	223.9 ± 16.5**	213.4 ± 10.2**	165.8 ± 9.0**	246.6 ± 16.6**	223.9 ± 16.5**
Uterus						
Proestrus						
Absolute (g)	0.658 ± 0.020 (5)	0.647 ± 0.070 (5)	0.599 ± 0.068 (6)	NE	0.632 ± 0.042 (3)	0.547 ± 0.085** (4)
Relative (g/100g B.W.)	0.267 ± 0.019 (5)	0.283 ± 0.029 (5)	0.279 ± 0.017 (6)	NE	0.298 ± 0.020 (3)	0.320 ± 0.037* (4)
Diestrus						
Absolute (g)	0.506 ± 0.031 (5)	0.491 ± 0.035 (5)	0.446 ± 0.010 (4)	0.171 ± 0.043** (10)	0.553 ± 0.075 (5)	0.420 ± 0.043 (4)
Relative (g/100g B.W.)	0.207 ± 0.022 (5)	0.225 ± 0.019 (5)	0.210 ± 0.005 (4)	0.103 ± 0.026** (10)	0.252 ± 0.032* (5)	0.247 ± 0.020 (4)
Ovary						
Absolute (g)	0.093 ± 0.004	0.090 ± 0.009	0.081 ± 0.011**	0.051 ± 0.009**	0.091 ± 0.013	0.069 ± 0.013**
Relative (g/100g B.W.)	0.038 ± 0.003	0.040 ± 0.006	0.038 ± 0.005	0.031 ± 0.004**	0.042 ± 0.006	0.040 ± 0.008
Pituitary						
Absolute (g)	0.014 ± 0.001	0.012 ± 0.002**	0.011 ± 0.001**	0.007 ± 0.002**	0.012 ± 0.002**	0.011 ± 0.001**
Relative (g/100g B.W.)	0.006 ± 0.000	0.005 ± 0.001	0.005 ± 0.000	0.004 ± 0.001**	0.005 ± 0.001	0.006 ± 0.001
Adrenals						
Absolute (g)	0.065 ± 0.008	0.065 ± 0.004	0.063 ± 0.008	0.048 ± 0.007**	0.063 ± 0.007	0.050 ± 0.009**
Relative (g/100g B.W.)	0.027 ± 0.003	0.029 ± 0.002	0.030 ± 0.004	0.029 ± 0.003	0.029 ± 0.003	0.030 ± 0.005
Thymus						
Absolute (g)	0.533 ± 0.089	0.435 ± 0.045	0.409 ± 0.059**	0.327 ± 0.061**	0.481 ± 0.082	0.358 ± 0.082**
Relative (g/100g B.W.)	0.216 ± 0.027	0.194 ± 0.016	0.192 ± 0.029	0.197 ± 0.032	0.222 ± 0.033	0.210 ± 0.045
Liver						
Absolute (g)	10.879 ± 1.105	10.637 ± 0.925	12.105 ± 1.087*	11.387 ± 0.931	8.126 ± 0.754**	6.238 ± 0.581**
Relative (g/100g B.W.)	4.414 ± 0.365	4.749 ± 0.135	5.670 ± 0.378**	6.864 ± 0.388**	3.751 ± 0.272**	3.665 ± 0.196**

a)Mean ± S.D.

*, **: Significantly different from the control group at $P < 0.05$ and 0.01, respectively.

NE : Not examined

Values in parentheses indicate the number of animals examined.

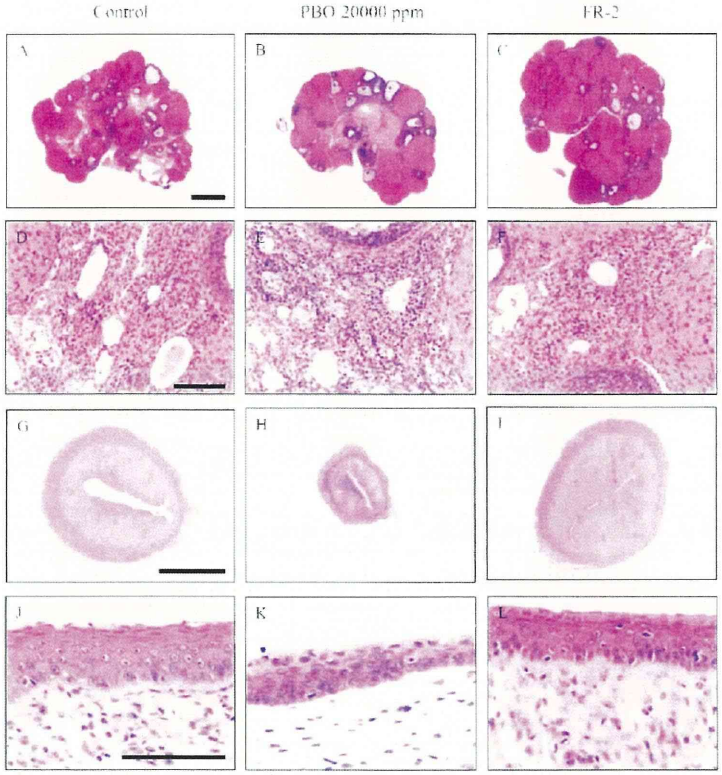

Fig. 4. Representative histopathology of the ovary, uterus and vagina at diestrus in experiment 1. Control ovary (A, D), 20,000 ppm group with numerous large, atretic follicles (*), decrease in newly formed corpora lutea and vacuolation of interstitial cells (B, E), and FR-2 without abnormality (C, F). Uterus of the control group (G), the 20,000 ppm group showing atrophy (H), FR-2 group showing no abnormalities (I). Vagina of the control group (J), the 20,000 ppm group showing thin and mucinous degeneration of the vaginal epithelium (K), and the FR-2 group showing no abnormalities (L). Bars = 1 mm (A, B, C, G, H, I), and 100 μm (D, E, F, J, K, L).

topathological findings.

Microscopic changes noted in the 20,000 ppm group are summarized in Fig. 4 and Table 4. The most pronounced was the severe atrophy of the uterus (Fig. 4H) with thinning and mucinous degeneration in the vaginal epithelium visible at a higher magnification (Fig. 4K). The ovaries in this group had numerous, large, atretic follicles with the most recent formed corpora lutea (Fig. 4B) and vacuolation of the interstitial cells (Fig. 4E). In the 5,000 and 10,000 ppm groups and the FR groups (Fig. 4C, F, I, L), there were no changes in the female reproductive tract. Centrilobular hypertrophy of the hepatocytes was observed in the 10,000 and 20,000 ppm groups (Table 4). No abnormalities were detected in the

Table 4. Incidence and grading of histopathologic findings (experiment 1).

Organ and findings	Piperonyl butoxide in the diet (ppm)				FR-1	FR-2
	0	5,000	10,000	20,000		
Ovary						
Increase in atretic follicle	0/10	0/10	0/10	5/10 (2)	0/8	0/8
Vacuolation, interstitial cell	0/10	0/10	0/10	10/10 (1-2)	0/8	0/8
Decrease/lack in newly formed corpora lutea	0/10	0/10	0/10	9/10 (1-2)	0/8	0/8
Uterus						
Atrophy	0/10	0/10	0/10	10/10 (4)	0/8	0/8
Vagina						
Mucinous degeneration	0/10	0/10	0/10	8/10 (1-2)	0/8	0/8
Thinning in the vaginal epithelium	0/10	0/10	0/10	10/10 (1-2)	0/8	0/8
Liver						
Hepatocellular hypertrophy, centrilobular	0/10	0/10	10/10 (1-2)	10/10 (2-3)	0/8	0/8

Incidence is given as total observations/ number of animals examined. Values in parentheses indicate grading or grading range as subjective severity scores : 1 = minimal, 2 = mild, 3 = moderate, 4= severe.

other organs in any of the groups.

Serum hormone levels

The serum E2 levels at diestrus in the 10,000 and 20,000 ppm groups were significantly lower than that of the control group (Fig. 5A). The serum LH levels at diestrus in the 20,000 ppm group were significantly higher than those in the control group (Fig. 5D). The serum inhibin levels at proestrus in the 10,000 ppm group were significantly lower than those of the control group (Fig. 5F). In the FR groups, the most notable change was an increase in corticosterone levels (Fig. 5G), and serum P4 and LH levels at proestrus were significantly higher and the serum FSH levels at both proestrus and diestrus were significantly lower than those of the control group (Fig. 5B, C, D). There was no significant difference in the PRL levels (Fig. 5E).

Experiment 2 (Anti-uterotrophic assay)

Body weight

The body weights in the 5,000, 10,000 and 20,000 ppm groups were reduced during the treatment period (Fig. 6). Final body weights in the 5,000, 10,000 and 20,000 ppm groups were about 95, 91 and 83% of the corresponding body weights at day 0.

Food consumption and chemical intake

The food consumption in the 10,000 and 20,000 ppm groups was lower than that in the NC group in the first 3 days (Fig. 7). The actual PBO intake in the 5,000, 10,000 and 20,000 ppm group was 283.9, 543.8 and 1342.1 mg/kg per day, respectively (Table 5). The chemical intake in each treatment group was about half of what was consumed by the matched treatment group in experiment 1.

Uterine weight

Both the wet and blotted absolute uterine weights in the 10,000 and 20,000ppm groups were significantly lower than those of the NC group (Fig. 8A). Relative uterine weights, however, showed a trend towards increase given the body weight reduction in these groups (Fig. 8B).

Measurement of uterine epithelial cell height

Histopathological measurement demonstrated that the uterine epithelial cell height in the 20,000 ppm group was significantly lower than that of the NC group (Fig. 9A, B).

Experiment 3 (Reporter gene assay)

Fig. 10 shows concentration response curve for the estrogen receptor antagonist activity of PBO and 4-hydroxytamoxifen (4OH-TAM), the active metabolite of tamoxifen, a known estrogen receptor antagonist. The IC50 was the concentration at which the transcription activity of 25pM E2 was reduced by 50%, in the concentration range showing more than 80% cell survival. The IC50 of PBO (2.24×10^{-5} M) was much higher than that of 4OH-TAM (3.11×10^{-10} M).

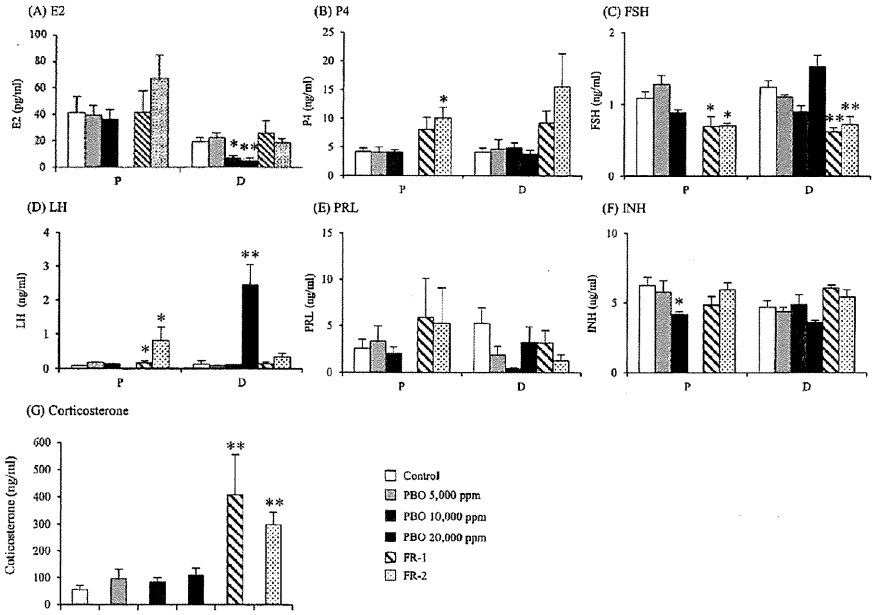

Fig. 5. Serum hormone levels in experiment 1. (A) 17β-estradiol (E2), (B) Progesterone (P4), (C) FSH, (D) LH , (E) Prolactin (PRL), (F) Inhibin α (INH) concentration at each estrus stage (P: proestrus, D: diestrus). (G) Mean serum corticosterone concentration. Data are represented as mean ± S.E.M. *, **: Significantly different from the 0 ppm group at $P < 0.05$ and 0.01, respectively.

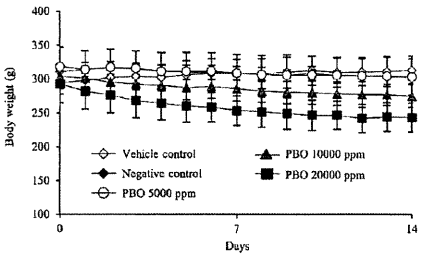

Fig. 6. Body weight curves in experiment 2 (mean ± S.D.).

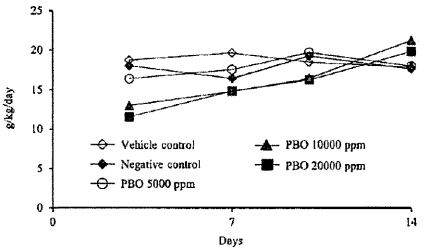

Fig. 7. Daily food intake in experiment 2 (mean ± S.D.).

Table 5. Achieves dose of PBO (experiment 2).

	Pyperonyl butoxide in diet (ppm)		
	5,000	10,000	20,000
	E2 1μg/kg	E2 1μg/kg	E2 1μg/kg
No. of animals	5	5	5
Intake of PBO (mg/kg bw/day)	283.93 ± 17.22[a)]	543.79 ± 75.34	1342.06 ± 225.68

[a)]Mean ± S.D.

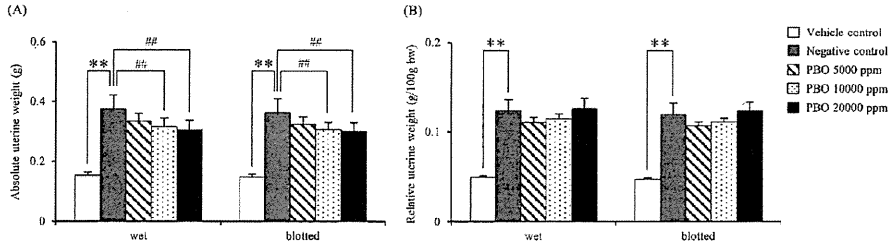

Fig. 8. Wet and blotted uterine weights in experiment 2. Data are represented absolute (A) and relative (B) uterine weights (mean ± S.D.), ** ; significantly different from the vehicle control group at $P < 0.01$, #, ## ; significantly different from the negative control group at $P < 0.05$, 0.01, respectively.

DISCUSSION

The present study investigated the effects of PBO on the female reproductive tract, focusing on the possibility that these are nonspecific effects related to the suppression of body weight gain by PBO. The most notable changes induced by PBO were estrous cycle disruption, uterine atrophy, and lowered serum E2 levels. Furthermore, *in vivo* and *in vitro* assays demonstrated that PBO has weak anti-estrogenic activity.

Estrous cycle disruption was present in both the PBO 20,000 ppm group and the FR-2 group in experiment 1. A previous report showed that rapid body weight reduction was responsible for the increased estrous cycle length in rats subjected to FR (Chapin *et al.*, 1993). However, the present study showed that the PBO group differed in the duration of the estrous cycle abnormalities from food restricted rats in the previous report and in the FR-2 group. The estrous cycles of the FR-2 group normalized once body weight gain recovering to increase, but prolonged diestrus continued in the 20,000 ppm PBO group even after body weight gain recovered to increase. These results suggest that prolonged diestrus in the PBO 20,000 ppm group may have resulted from something other than reduced body weight. This idea was further supported by the significant decrease in the relative weights of the reproductive organs in the PBO 20,000 ppm group and differences in the patterns of reproductive hormone levels between the PBO and FR groups. Elevated corticosterone is a known stress response induced by hunger and limited access to food (Kasanen *et al.*, 2009). High-dose PBO treatment did not affect corticosterone levels whereas the FR groups showed increased corticosterone levels. These results indicate that the reproductive effects of reduced body weight in the FR group may be related to stress, whereas this indicator of stress was not present in the PBO group under the present study conditions.

Histopathological changes induced by high-dose PBO treatment, including severe uterine atrophy, vaginal thinning with mucification, and ovarian changes such as an increased number of atretic follicles and decreased numbers of recent corpora lutea, were typical of the hypoestrogenic or anti-estrogenic state resulting in anovulation. These changes were not observed in the FR-2 group. Our hormone measurements in experiment 1 revealed that both the 10,000 and 20,000 ppm PBO groups were in a

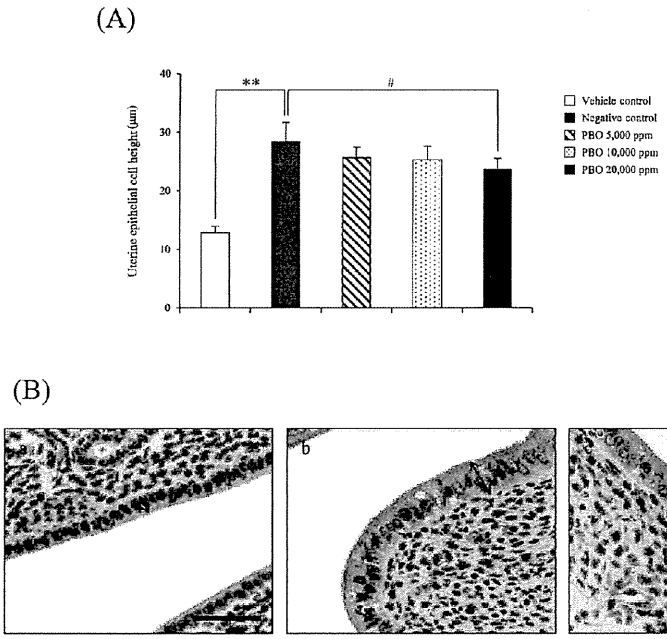

Fig. 9. Histopathological examination of uterus in experiment 2. (A) Uterine epithelial cell height (mean ± S.D.), **; significantly different from the vehicle control group at $P < 0.01$, #; significantly different from the negative control group at $P < 0.01$. (B) Histopathology of uterine epithelial cells. (a) vehicle control group, (b) negative control group, (c) 20,000 ppm group. Double-headed arrows indicate uterine epithelial cell heights. Bars = 50μm.

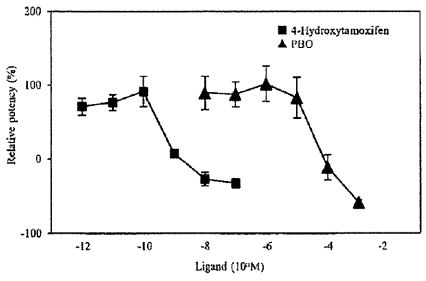

Fig. 10. Concentration response curve of the ER α reporter gene assay in experiment 3 (mean ± S.D.).

hypoestrogenic state at diestrus when E2 levels are normally gradually increasing, indicating that high-dose PBO treatment may induce a hypoestrogenic state although a clear mechanism was not determined in the present study. E2 is metabolized by cytochrome P450s (CYPs) in the liver and other organs and tissues (Dannan *et al.*, 1986; Hammond *et al.*, 1997; Zhu and Conney, 1998; Yoshida *et al.*, 2004). PBO causes liver hypertrophy and induces CYP 1A and 2B mRNA expression (Muguruma *et al.*, 2006), which may affect E2 metabolism. In contrast, treatment with 2,3,7,8-tetrachlorodibenzo-p-dioxin (TCDD), an aryl hydrocarbon receptor (AhR) agonist, induces CYP1A and 1B mRNA expression without affecting E2 levels (Shiverick and Muther, 1982; DeVito *et al.*, 1992). Another possible mechanism of hypoestrogenism is the

inhibition of steroidogenesis in the ovary; this possibility was not investigated in the present study. Further analysis is needed to fully elucidate the effects of PBO on E2 metabolism in the liver and steroidogenesis in the ovary.

The anti-estrogenic effects of PBO are another possible cause of estrous cycle disruption and atrophic changes (Tsujioka *et al.*, 2009). A reporter gene assay indicated that PBO has anti-estrogenic effects, but they were much weaker than those of the estrogen receptor antagonist 4OH-TAM. In anti-uterotrophic study (experiment 2), the significant decrease in absolute uterine weight induced by E2 and PBO treatment groups was likely due to the weak anti-estrogenic effects of PBO, because the relative uterine weight was not decreased due to body weight depression in the PBO group. In addition, the statistically significant decrease in the heights of uterine epithelial cells in the 20,000 ppm group compared with the E2 only group also supports the idea that PBO has anti-estrogenic effects, because uterine epithelial cell height is a well-established indicator of estrogenicity (Cho *et al.*, 2003; Diel *et al.*, 2002).

In conclusion, high-dose PBO treatment resulted in marked uterine atrophy, vaginal atrophy, and ovarian changes resulting in anovulatory status in rats. These changes were independent of body weight depression, and may result from a hypoestrogenic state and anti-estrogenic effects of PBO. However, the levels of PBO used in the present study were very high. Acceptable daily intake (ADI) of PBO was set at 0.2 mg/kg body weight by JMPR in 1995 (FAO, 2011), so margin of exposure is approximately 5,000 fold. Therefore, these effects are not considered to be relevant to humans at exposure levels present in the environment.

ACKNOWLEDGMENTS

The authors are very grateful to Ms. Tomomi Morikawa, Ms. Ayako Kaneko and Ms. Yoshimi Komatsu for their excellent technical assistance. We also appreciate Drs. Satoshi Furukawa, Koji Usuda and Masayoshi Abe (Toxicology Group, Toxicology and Environmental Science Department, Biological Research Laboratories, Nissan Chemical Industry Co., Ltd.) for their helpful suggestions. This study was partly supported by Health and Labour Science Research Grants, Research on Risk of Chemical Substances [H25-Toxicol-003], Ministry of Health, Labour and Welfare.

REFERENCES

Butler, W.H., Gabriel, K.L., Osimitz, T.G. and Preiss, F.J. (1998): Oncogenicity studies of piperonyl butoxide in rats and mice. Hum. Exp. Toxicol., 17, 323-330.

Chapin, R.E., Gulati, D.K., Barnes, L.H and Teague, J.L. (1993): The effects of feed restriction on reproductive function in Sprague-Dawley rats. Fundam. Appl. Toxicol., **20**, 23-29.

Cho, S.D., Kim, J.H., Kim, D.Y., Lee, Y.S. and Kang, K.S. (2003): Pre-validation study for OECD enhanced test guideline 407 protocol by gavage for 4 weeks using propylthiouracil and tamoxifen. Toxicol. Lett., 144, 195-204.

Dannan, G.A., Porubek, D.J., Nelson, S.D., Waxman, D.J. and Guengerich, E.P. (1986): 17 β-estradiol 2- and 4-hydroxylation catalyzed by rat hepatic cytochrome P-450: roles of individual forms, inductive effects, developmental patterns, and alterations by gonadectomy and hormone replacement. Endocrinology, 118, 1952-1960.

DeVito, M.J., Thomas, T., Martin, E., Umbreit, T.H. and Gallo, M.A. (1992): Antiestrogenic action of 2,3,7,8-tetrachlorodibenzo-p-dioxin: tissue-specific regulation of estrogen receptor in CD1 mice. Toxicol. Appl. Pharmacol., 113, 284-292.

Diel, P., Schmidt, S. and Vollmer, G. (2002): *In vivo* test systems for the quantitative and qualitative analysis of the biological activity of phytoestrogens. J. Chromatogr. B Anal. Technol. Biomed. Life Sci., 777, 191-202.

Food and Agriculture Organization of the United Nations (FAO) (2011): FAO specifications and evaluations for agricultural pesticides. http://www.fao.org/fileadmin/templates/agphome/documents/Pests_Pesticides/ Specs/piperonyl_butoxide_2011.pdf

Franklin, M.R. (1972): Inhibition of hepatic oxidative xenobiotic metabolism by piperonyl butoxide. Biochemical Pharmacology, 21, 3287-3299.

Fujitani, T., Ando, H., Fujitani, K., Ikeda, T., Kojima, A., Kubo, Y., Ogata, A., Oishi, S., Takahashi, H., Takahashi, O. and Yoneyama, M. (1992): Sub-acute toxicity of piperonyl butoxide in F344 rats. Toxicology, 72, 291-298.

Hamada, T., Watanabe, G., Kokuho, T., Taya, K., Sakamoto, S., Hasegawa, Y., Miyamoto, K. and Igarashi, M. (1989): Radioimmunoassay of inhibin in various mammals. J. Endocrinol., 122, 697-704.

Hammond, D.K., Zhu, B.T., Wang, M.Y., Ricci, M.J. and Liehr, J.G. (1997): Cytochrome P450 metabolism of estradiol in hamster liver and kidney. Toxicol. Appl. Pharmacol., 145, 54-60.

Kasanen, I.H., Inhilä, K.J., Vainio, O.M., Kiviniemi, V.V., Hau, J., Scheinin, M., Mering, S.M. and Nevalainen, T.O. (2009): The diet board: welfare impacts of a novel method of dietary restriction in laboratory rats. Lab. Anim., 43, 215-223.

Muguruma, M., Nishimura, J., Jin, M., Kashida, Y., Moto, M., Takahashi, M., Yokouchi, Y. and Mitsumori, K. (2006): Molecular pathological analysis for determining the possible mechanism of piperonyl butoxide-induced hepatocarcinogenesis in mice. Toxicology, 228, 178-187.

Muguruma, M., Unami, A., Kanki, M., Kuroiwa, Y., Nishimura, J., Dewa, Y., Umemura, T., Oishi, Y. and Mitsumori, K. (2007): Possible involvement of oxidative stress in piperonyl butoxide induced hepatocarcinogenesis in rats. Toxicology, 236, 61-75.

Phillips, J.C., Price, R.L., Cunninghame, M.E., Osimitz, T.G., Cockburn, A., Gabriel, K.L., Preiss, F.J., Butler, W.H. and Lake, B.G. (1997): Effect of piperonyl butoxide on cell replication and xenobiotic metabolism in the livers of CD-1 mice and F344 rats. Fundam. Appl. Toxicol., 38, 64-74.

Shiverick, K.T. and Muther, T.F. (1982): Effects of 2,3,7,8-tetrachlorodibenzo-p-dioxin on serum concentrations and the uterotrophic action of exogenous estrone in rats. Toxicol. Appl.

Pharmacol., 65, 170-176.
Takahashi, O., Oishi, S., Fujitani, T., Tanaka, T. and Yoneyama, M. (1994): Chronic toxicity studies of piperonyl butoxide in F344 rats: induction of hepatocellular carcinoma. Fundam. Appl. Toxicol., 22, 293-303.
Takeyoshi, M., Yamasaki, K., Sawaki, M., Nakai, M., Noda, S. and Takatsuki, M. (2002a): The efficacy of endocrine disruptor screening tests in detecting anti-estrogenic effects downstream of receptor-ligand interactions. Toxicol. Lett., 126, 91-98.
Takeyoshi, M., Kuga, N. and Yamasaki, K. (2002b): Development of a high-performance reporter plasmid for detection of chemicals with androgenic activity. Arch. Toxicol., 77, 274-279.
Taya, K., Mizokawa, T., Matsui, T. and Sakamoto, S. (1983): Induction of superovulation in prepubertal female rats by anterior pituitary transplants. J. Reprod. Fertil., 69, 265-270.
Taya, K., Watanabe, G. and Sasamoto, S. (1985): Radioimmunoassay for progesterone, testosterone and estradiol-17β using 125I-iodohistamine radioligands. Jpn. J. Anim. Reprod., 31,186-197.
Terry, K.K., Chatman, L.A., Foley, G.L., Kadyszewski, E., Fleeman, T.L., Hurtt, M.E. and Chapin, R.E. (2005): Effects of Feed Restriction on Fertility in Female Rats. Birth. Defects Res. B Dev. Reprod. Toxicol., 74, 431-441.
Tsujioka, S., Ban, Y., Wise, L.D., Tsuchiya, T., Sato, T., Matsue, K., Ikeda, T., Sasaki, M. and Nishikibe, M. (2009): Collaborative work on evaluation of ovarian toxicity. 3) Effects of 2- or 4-week repeated-dose toxicity and fertility studies with tamoxifen in female rats. J. Toxicol. Sci., 34, SP43-SP51.
Westwood, F.R. (2008): The female rat reproductive cycle: A practical histological guide to staging. Toxicol. Pathol., 36, 375-384.
Yoshida, M., Katashima, S., Ando, J., Tanaka, T., Uematsu, F., Nakae, D. and Maekawa, A. (2004): Dietary indole-3-carbinol promotes endometrial adenocarcinoma development in rats initiated with N-ethyl-N'-nitro-N-nitrosoguanidine, with induction of cytochrome P450s in the liver and consequent modulation of estrogen metabolism. Carcinogeneisis, 25, 2257-2264.
Yoshida, M., Sanbuissyo, A., Hisada, S., Takahashi, M., Ohno, Y. and Nishikawa, A. (2009): Morphological characterization of the ovary under normal cycling in rats and its viewpoints of ovarian toxicity detection. J. Toxicol. Sci., 34, Suppl. 1, SP189-SP97.
Yuan, Y.D. and Foley, G.L. (2002): Female Reproductive System. In Handbook of Toxicologic Pathology. Second Edition (Haschek, W.M., Rousseaux, C.G., Walling, M.A. eds.), pp847-894. Academic Press, San-Diego.
Zhu, B.T. and Conney, A.H. (1998): Functional role of estrogen metabolism in target cells: review and perspectives. Carcinogenesis, 19, 1-27.